

# Generalized Oberst beam method for measuring viscoelastic parameters of layered composite components

A. DOBRUCKI<sup>1</sup>), R. BOLEJKO<sup>1</sup>), P. NIERADKA<sup>1,2</sup>), A. KLIMEK<sup>1</sup>)

<sup>1</sup>) *Chair of Acoustics, Multimedia and Signal Processing, Faculty of Electronics, Photonics and Microsystems, Wrocław University of Science and Technology, Wybrzeże Wyspiańskiego 27, 50-370 Wrocław, Poland, e-mail: andrzej.dobrucki@pwr.edu.pl (corresponding author)*

<sup>2</sup>) *KFB Acoustics, Mydlana 7, 51-502 Wrocław, Poland*

THIS PAPER PROPOSES TWO NEW METHODS of measuring the viscoelastic parameters of materials. The methods are based on the composite beams' resonant frequencies measurement. The Young moduli and loss factors of the components are determined by measuring the frequency response of a composite beam twice, each time with different layer thickness ratios. A system of two equations is obtained, from which Young's moduli of the composite components are calculated. Similarly, two obtained equations determine the loss factors. The results obtained by the proposed methods are compared with those obtained by standard methods and then validated by experiments and FEM simulations. It was noted that the developed models, as well as the standard ones, are highly sensitive to the precision of the samples (material trimming and the way of joining the composite elements). The proposed methods prove to have an advantage over the standard ones in the matter of more frequent measurement criterion fulfilment. The acknowledged criterion represents the existence of a sensible solution insensitive to measurement errors. This criterion, which assures that the results are not prone to errors (for example negative loss factors) is met in 100% of cases in one of the methods, compared to 65% for standard methods.

**Key words:** viscoelastic materials, composites, Young modulus, loss factor, beam resonance, Oberst beam method.



Copyright © 2023 The Authors.

Published by IPPT PAN. This is an open access article under the Creative Commons Attribution License CC BY 4.0 (<https://creativecommons.org/licenses/by/4.0/>).

## 1. Introduction

IN MODERN ENGINEERING PROBLEMS, the cost of making physical prototypes of products could be very high. When there is a need to modify a particular product component, assessing the impact of this change on the whole system behaviour is an important task (e.g. an increase in noise generation or vibration levels). In this case, the so-called virtual prototyping involving numerical simulations' execution on a calibrated model of the product or machine under test is much more cost-effective. An important factor determining the high quality of the vibro-acoustic model is the accurate knowledge of the considered materials' mechanical

parameters. The literature provides numerous methods for the determination of viscoelastic parameters. These include methods based on ultrasonic measurements [1], impulse methods [2], Dynamic Mechanical Analysis (DMA) [3], Dynamic Mechanical Thermal Analysis (DMTA) [4], Broadband Viscoelastic Spectroscopy (BVS) [5], transfer function methods [6–8], and others (e.g. the material loss factor can be determined using the reverberation time method [9], modal curve fitting [10], or the SEA statistical method [11]). Each of the mentioned procedures has individual advantages and disadvantages. This paper focuses on the methods that take advantage of the relationship between the materials' mechanical parameters and the resonant frequencies of beams made from given materials [12–18]. The resonance method (Oberst beam method) is standardized by ASTM in [19] as well as by other standardization organizations [20, 21] in equivalent documents. Hitherto, some authors raised the issue of the mentioned method course, i.e. the excitation and sensor effect [22, 23]. The issue of measuring non-magnetic materials with the Oberst beam method using non-contact exciters was raised, and solutions based on utilizing lightweight magnetic particles or discs was proposed [15]. Other researchers pointed out the effect of many set-up and post-processing parameters on the final results [16, 17]. Those parameters include frequency resolution in frequency responses, the distance between the beam tip and the electromagnetic exciter, the excitation amplitude, and sample preparation. A different study investigates the effect of sample thickness on the damping loss factor [18].

There also have been publications removing the requirement for non-contact excitation in this method [24]. A great advantage of resonance methods is the relatively simple testing methodology. On the other hand, one of the disadvantages of resonance methods is the poor numerical conditioning that can occur when the strict conditions set in [19] are unmet. This situation can force the tester to prepare multiple samples of the same composite to find the ones that will produce a physically meaningful result. In this article, the derived methods are related to those found in the standard [19]. Measurements were performed on a set of composite beams in order to compare the existing and proposed methods.

The structure of the paper is as follows:

Section 2 discusses the existing methods for measuring viscoelastic parameters based on the measurement of beam resonance frequencies and the width of resonance curves. Moreover, the section proposes two new methods.

Section 3 describes the numerical validation run, including an assessment of the influence of the accuracy of preparing samples on the obtained results.

Section 4 presents details of the carried out experiments.

Section 5 discusses the results of the tests, in particular, the influence of the adhesive as well as the parameters and type of the core (also a core made of PVC, which is not recommended in the standards) on the determined rubber

jacket parameter. Each of the mentioned factors was considered separately in the context of new and existing methods (except for the influence of the adhesive, which was considered only for the standard method).

Section 6 summarizes the carried out research and presents the resulting conclusions.

In this article, the following words are used interchangeably: jacket, coating, shell, sheath and sheathing.

## 2. Theory

The main objective of these measurement methods is to determine the viscoelastic parameters of materials unable to form a self-supporting beam due to their limpness. One solution may be to use the quasi-static method [25], where both beam ends are clamped. An alternative method discussed in this article is to use base beams made of a rigid material (e.g., steel), which forms a stable structure with a tested flaccid material (e.g., rubber). Therefore, the resulting composite consists of a base beam (core) acting as the supporting element and one or two shells made of viscoelastic material being the main testing element. Consequently, the frequency response of the composite beams (and possibly the cores themselves) could be assessed during the laboratory measurements. Frequency response provides two main quantities for each beam resonance: its frequency and half power bandwidth. It is then, by using the developed mathematical models, possible to extract the coating parameters.

In the first part of this section, a basic model for determining the viscoelastic parameters of the base beam and the effective viscoelastic parameters of the composite beam are discussed.

In the second part of the section, models known from ASTM E-756 [19] for the determination of shell viscoelastic parameters are presented.

In the third part, new methods that can be an alternative to those described in the standards are introduced. By using these methods, one can determine the material parameters of both the base beam and the coating.

### 2.1. Basis of the method

The method involves measuring the resonant frequencies of a rectangular cross-section beam clamped at one end and free at the other. The successive resonant frequencies of the beam are expressed by the formula:

$$(2.1) \quad f_i = \frac{\gamma_i}{l^2} \sqrt{\frac{EI}{\rho_S}}, \quad i = 1, 2, 3, \dots,$$

$$\gamma_1 = 0.55966, \quad \gamma_2 = 3.5074, \quad \gamma_3 = 9.8209, \quad \gamma_4 = 19.2450, \dots,$$

where:  $l$  – beam length,  $E$  – Young’s modulus,  $r_S$  – surface density,  $I$  – moment of inertia of the cross section.

If the beam is homogeneous, Young’s modulus and density are parameters of the base material. The moment of inertia is then:

$$(2.2) \quad I = bh^3/12,$$

where:  $b$  – width,  $h$  – thickness of the beam.

The surface density is given by the formula:

$$(2.3) \quad \rho_S = \rho \cdot S,$$

where:  $\rho$  – density of the beam material,  $S$  – cross section area.

In the following section, expressions for the  $EI$  and surface density of beams  $\rho_S$  with a sandwich structure are derived. These parameters, known as effective parameters, depend on the thickness and material parameters of the individual layers.

Knowing the density and geometrical parameters of the beam, it is possible to determine Young’s modulus by measuring any resonance frequency (usually the first one). The resonant frequency is defined as the frequency at which the local maximum of the deflection amplitude of the flexural stimulated beam occurs (Fig. 1).

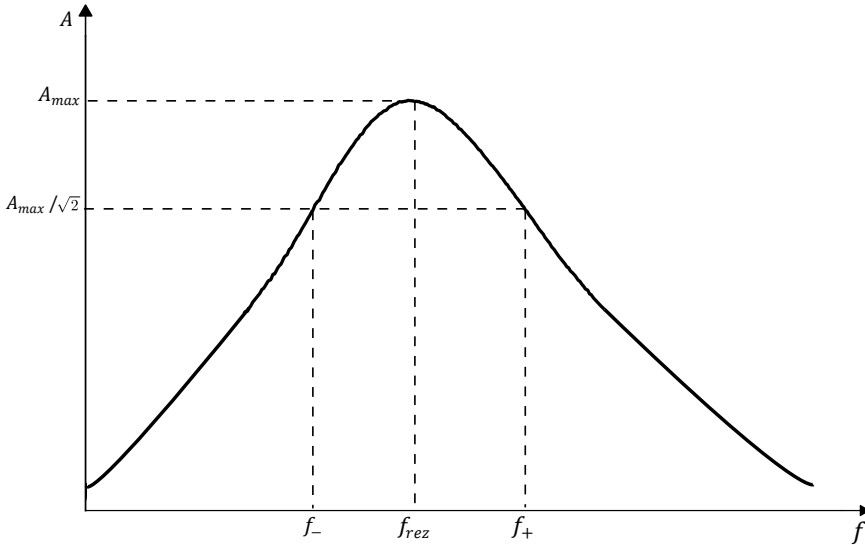


FIG. 1. Resonance curve.

From Eq. (2.1), taking into account (2.2) and (2.3), the Young modulus could be represented as:

$$(2.4) \quad E = 12 \frac{f_i^2 l^4 \rho}{\gamma_i^2 h^2}.$$

Young's modulus of lossy materials is a complex quantity  $\underline{E} = E(1 + j\eta)$ . The quantity  $\eta$  is called the loss factor. It usually has very low value, even for highly lossy materials, so the real quantity  $E$  can be taken as Young's modulus. The value of the loss factor is evaluated by measuring two frequencies below and above the resonance frequency so that the vibration amplitude decreases to  $A_{max}/\sqrt{2}$ . These frequencies are denoted in Fig. 1 as  $f_-$  and  $f_+$ . The loss factor is calculated from the formula:

$$(2.5) \quad \eta = \frac{f_+ - f_-}{f_i}.$$

Both  $E$  and  $\eta$  could depend on frequency.

## 2.2. Oberst and modified Oberst methods for the identification of damping material parameters

In this article, we examine two of the three models proposed in the ASTM standard.

The first model is the Oberst Beam Model (referred to in this article as O), where the composite beam consists of a core and a sheathing attached to one side of the beam. The second model is the Modified Oberst Beam Model (referred to in this article as MO), where the composite beam consists of a core and sheathing attached to both sides of the beam.

The first step of the standardized methods is to determine the natural frequencies and the widths of the resonance curves of the base (sometimes called bare) beam. Then, by using the model presented in the previous section, Young's modulus and the core loss factor are calculated. The next step is to repeat the described procedure for the composite beam to obtain composite Young's modulus and the loss factor. With these data, one can determine the parameters of the shell using the relationships presented in the standard. To avoid numerical errors, the following condition must be met:

$$(2.6) \quad \frac{f_{ieff}^2}{f_{ib}^2} \left( 1 + \frac{\rho_2 h_2}{\rho_1 h_1} \right) \geq 1.01,$$

where  $f_{ieff}$  is the effective  $i$ -th resonant frequency of the composite,  $f_{ib}$  is the  $i$ -th resonant frequency of the bare beam, and  $\rho_2$  and  $h_2$  are, respectively, the density and thickness of the sheathing for the O method and the density and thickness of both layers of the sheathing for the MO method. The product  $\rho h$  is the surface density.

## 2.3. Identification of the parameters of damping materials – proposed methods

In this section, alternative methods to the standard are derived for determining the viscoelastic parameters of materials using flexural vibrations of composite

beams. Unlike the methods described in the ASTM standard, the proposed ones do not require a separate core measurement.

The first approach (referred to here as PM1; Proposed Method 1) is equivalent to the standard MO method. Unlike the MO method, the PM1 method measures a beam twice, each time with a double-sided shell, but for two different shell thicknesses. Two systems of linear equations are obtained. The first system delivers Young's modulus of the base beam and jacket material, while the second system gives the corresponding loss factors.

The second method (called here PM2; Proposed Method 2) is equivalent to the standard method O. In contrast to method O, in the PM2, the beam with one-sided sheathing is measured twice for two different sheathing thicknesses. One system of nonlinear equations and one system of linear equations are obtained. The first system provides Young's modulus of the base beam and the sheathing, while the second system determines the loss factors of the base beam and the sheathing.

**2.3.1. The PM1 method.** The geometry of the problem is as follows. A beam of length  $l$  is made of a composite consisting of three layers. The middle layer (the core of the composite) has a thickness of  $h_1$  and is covered on both sides by a material with a thickness of  $h_2/2$  on each side, constituting the sheathing of the composite (Fig. 2).

Figure 2 shows the  $z$ -axis. The zero point of this axis is located at the center of the beam's cross-section. The effective value of the product of  $EI$  is determined from the formula:

$$\begin{aligned}
 (2.7) \quad (EI)_{eff} &= \int_{-\frac{h_1+h_2}{2}}^{\frac{h_1+h_2}{2}} E(z)z^2b \, dz \\
 &= E_2b \int_{-\frac{h_1+h_2}{2}}^{-\frac{h_1}{2}} z^2 \, dz + E_1b \int_{-\frac{h_1}{2}}^{\frac{h_1}{2}} z^2 \, dz + E_2b \int_{\frac{h_1}{2}}^{\frac{h_1+h_2}{2}} z^2 \, dz,
 \end{aligned}$$

where  $E_1$  and  $E_2$  are Young's moduli of the composite core and sheathing, respectively. After calculating and ordering the integrals, the following is obtained:

$$\begin{aligned}
 (2.8) \quad (EI)_{eff} &= \frac{bh_2^3}{12} \left[ E_2 \left( 3 \frac{h_1^2}{h_2^2} + 3 \frac{h_1}{h_2} + 1 \right) + E_1 \frac{h_1^3}{h_2^3} \right] \\
 &= \frac{bh_2^3}{12} \left[ E_2 \left( \frac{h_1}{h_2} + 1 \right)^3 + \left( E_1 - E_2 \right) \frac{h_1^3}{h_2^3} \right].
 \end{aligned}$$

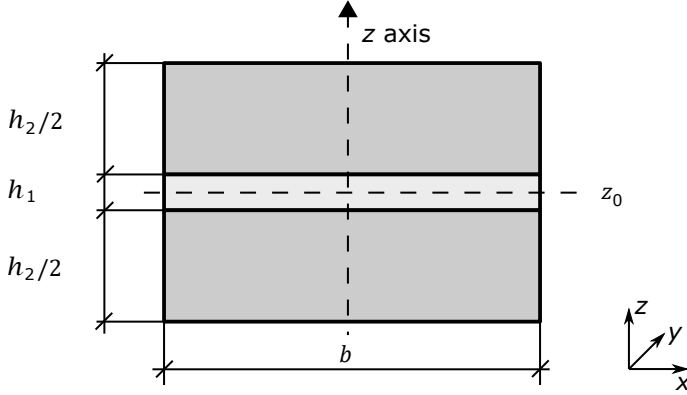


FIG. 2. Cross-section through a symmetric triple-layer composite beam.

The effective value of the product  $\rho S$  is:

$$(2.9) \quad (\rho S)_{eff} = \rho_1 b h_1 + \rho_2 b h_2.$$

Inserting (2.8) and (2.9) into Eq. (2.1) for the  $i$ -th resonant frequency, one obtains:

$$(2.10) \quad f_i = \frac{\gamma_i}{l^2} \left( \sqrt{\frac{EI}{\rho S}} \right)_{eff} = \frac{\gamma_i}{\sqrt{12}} \frac{h_2}{l^2} \sqrt{\frac{E_2 \left( 3 \frac{h_1^2}{h_2^2} + 3 \frac{h_1}{h_2} + 1 \right) + E_1 \frac{h_1^3}{h_2^3}}{\rho_1 \frac{h_1}{h_2} + \rho_2}}.$$

By measuring the resonant frequency of the beam twice, for two different sheathing thicknesses  $h_2$  and  $h'_2$ , a system of two linear equations is obtained, from which the values of  $E_1$  and  $E_2$  are determined.

Let us assign  $h_1/h_2$  by  $\kappa$ , and  $h_1/h'_2$  by  $\kappa'$ . Then, the system of equations has the form:

$$(2.11) \quad \begin{cases} \kappa^3 E_1 + (3\kappa^2 + 3\kappa + 1) E_2 = A \kappa^2 f_i^2 (\rho_1 \kappa + \rho_2), \\ \kappa'^3 E_1 + (3\kappa'^2 + 3\kappa' + 1) E_2 = A \kappa'^2 f_i^2 (\rho_1 \kappa' + \rho_2), \end{cases}$$

where:

$$A = \frac{12l^4}{\gamma_i^2 h_1^2}.$$

The principal determinant of this system of equations is:

$$(2.12) \quad \begin{aligned} \Delta &= \kappa^3 (3\kappa'^2 + 3\kappa' + 1) - \kappa'^3 (3\kappa^2 + 3\kappa + 1) \\ &= (\kappa - \kappa') [3\kappa^2 \kappa'^2 + \kappa \kappa' (3\kappa + 3\kappa' + 1) + (\kappa^2 + \kappa'^2)]. \end{aligned}$$

Because  $h'_2 > h_2$  then  $\kappa > \kappa'$  and formula (2.12) is always positive.

The determinants obtained by replacing respectively the 1st and the 2nd column of the main matrix by the free column (on the right-hand side of the system (2.11)) are:

$$(2.13a) \quad \Delta_1 = A[\rho_1(f_i^2 \kappa^3 - f_i'^2 \kappa'^3) + (3\rho_1 \kappa \kappa' + \rho_2)(f_i^2 \kappa^2 - f_i'^2 \kappa'^2) \\ + 3\kappa \kappa'(\rho_1 \kappa \kappa' + \rho_2)(f_i^2 \kappa - f_i'^2 \kappa') + 3\rho_2 \kappa^2 \kappa'^2 (f_i^2 - f_i'^2)],$$

$$(2.13b) \quad \Delta_2 = A[\rho_1 \kappa^3 \kappa'^3 (f_i'^2 - f_i^2) + \rho_2 \kappa^2 \kappa'^2 (f_i'^2 \kappa - f_i^2 \kappa')].$$

Young's moduli are calculated from the formulae:

$$(2.14) \quad E_1 = \frac{\Delta_1}{\Delta}, \quad E_2 = \frac{\Delta_2}{\Delta}.$$

When  $h_2' > h_2$  and  $\kappa' < \kappa$ , then the eigenfrequencies are  $f_i' < f_i$ . Then  $\Delta_1 > 0$  and also Young's modulus of the sheathing  $E_1 > 0$ . Of course, Young's modulus  $E_2$  is also greater than zero, but the calculated value of  $\Delta_2$  can be negative because of measurement errors. The following condition must be fulfilled for the value  $\Delta_2$  to be positive:

$$(2.15a) \quad \rho_1 \kappa^3 \kappa'^3 (f_i'^2 - f_i^2) + \rho_2 \kappa^2 \kappa'^2 (f_i'^2 \kappa - f_i^2 \kappa') > 0$$

or

$$(2.15b) \quad \rho_2 (f_i'^2 \kappa - f_i^2 \kappa') > \rho_1 \kappa \kappa' (f_i'^2 - f_i^2)$$

or

$$(2.15c) \quad \rho_2 \left( \frac{f_i'^2}{\kappa'} - \frac{f_i^2}{\kappa} \right) > \rho_1 (f_i'^2 - f_i^2),$$

$$(2.15d) \quad \frac{\rho_1 h_1 + \rho_2 h_2}{\rho_1 h_1 + \rho_2 h_2'} f_i^2 < f_i'^2 < f_i^2.$$

When  $h_2 = 0$  (bare beam) then  $1/\kappa = 0$ , and the sheathing appears only in the second Eq. (2.11) ( $h_2' > 0$ ), the formula (2.15c) has the form:

$$(2.16a) \quad \rho_2 \frac{h_2'}{h_1} f_i'^2 > \rho_1 (f_i'^2 - f_i^2).$$

After transformations the result is:

$$(2.16b) \quad \frac{f_i'^2}{f_i^2} \left( \frac{\rho_2}{\rho_1} \frac{h_2'}{h_1} + 1 \right) > 1,$$

which is the requirement (2.6) of the ASTM standard [19]. The formula (2.15c) is therefore a generalized condition from the standard.

To ensure that the sheath material in the measurements is the same, often  $h'_2 = 2h_2$ , which is obtained by sticking together two layers cut from the same sheet of material. Then  $\kappa' = \kappa/2$  and condition (2.15c) has the form of:

$$(2.17) \quad \frac{\rho_2}{\rho_1} \frac{h_2}{h_1} (2f_i'^2 - f_i^2) > f_i^2 - f_i'^2.$$

In this paper, the value  $h'_2$  was chosen as double of  $h_2$ . Note that there is no beam width in Eq. (2.10). However, the densities of the two materials are required and must be determined by other means, for example by weighting the two samples. In the standard modified Oberst beam method condition (2.16b) is relatively often not fulfilled, whereas in the PM1 method condition (2.17) was fulfilled in all cases. This is an undoubted advantage of the proposed methods.

When the composite form of Young's modulus for both materials is taken, the effective loss factor of the composite is given by the formula:

$$(2.18) \quad \eta_{eff} = \frac{E_2 \eta_2 \left( 3 \frac{h_1^2}{h_2^2} + 3 \frac{h_1}{h_2} + 1 \right) + E_1 \eta_1 \frac{h_1^3}{h_2^3}}{E_2 \left( 3 \frac{h_1^2}{h_2^2} + 3 \frac{h_1}{h_2} + 1 \right) + E_1 \frac{h_1^3}{h_2^3}}.$$

Once Young's moduli have been determined, two values of the effective loss factor for two different ratios  $h_1/h_2$  are determined by measuring the widths of the resonance curves, with the desired loss factors of the composite components then being obtained from the system of equations.

**2.3.2. The PM2 method.** The geometry of the problem is as follows. A beam of length  $l$  is made of a composite consisting of two layers. The upper layer is made of material with Young's modulus  $E_1$ , and its thickness is  $h_1$ . The lower layer is made of material with Young's modulus  $E_2$ , and its thickness is  $h_2$  (Fig. 3).

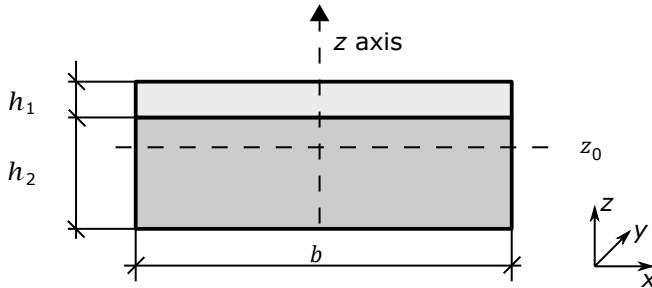


FIG. 3. Cross-section through a double-layer composite beam.

The  $z$ -axis is shown in Fig. 3. The zero point of this axis should lie in the neutral plane perpendicular to the  $z$ -axis, below which the planes are in compression during deflection, and above which they are in tension, or vice versa.

The neutral plane is bent, but not compressed or stretched. The point lying on the  $z$ -axis and on the neutral plane is denoted in Fig. 3 as  $z_0$ . The question of the deflection of a two-layer beam, or generally of a multilayer beam asymmetric about the  $z$ -axis, is more complex than that of a three-layer symmetric beam, because the value  $z_0$  is a priori unknown and must be determined.

Let us place the zero point on the  $z$  axis at the junction of two materials. The effective value of the  $EI$  product is:

$$(2.19) \quad (EI)_{eff} = b \int_{-h_2}^{h_1} E(z)(z - z_0)^2 dz \\ = b \left[ E_1 \int_0^{h_1} (z - z_0)^2 dz + E_2 \int_{-h_2}^0 (z - z_0)^2 dz \right].$$

After calculating the integrals and ordering the expressions with respect to the  $z_0$  powers, one obtains:

$$(2.20) \quad (EI)_{eff} = \frac{b}{3} [3(E_1 h_1 + E_2 h_2) z_0^2 - 3(E_1 h_1^2 - E_2 h_2^2) z_0 + (E_1 h_1^3 + E_2 h_2^3)].$$

This value is determined from the minimum value condition relative to  $z_0$ . By calculating the derivative and comparing it to zero:

$$(2.21) \quad \frac{d(EI)_{eff}}{dz_0} = b[2(E_1 h_1 + E_2 h_2) z_0 - (E_1 h_1^2 - E_2 h_2^2)] = 0$$

from which the value of  $z_0$  equals:

$$(2.22) \quad z_0 = \frac{1}{2} \cdot \frac{E_1 h_1^2 - E_2 h_2^2}{E_1 h_1 + E_2 h_2}.$$

The quantity  $z_0$  can be positive or negative depending on the sign of the numerator of expression (2.22). Inserting  $z_0$  from Eq. (2.22) into Eq. (2.20) gives, after ordering, an expression for  $(EI)_{eff}$ , in which all quantities are known:

$$(2.23) \quad (EI)_{eff} = \frac{b}{12} \cdot \frac{E_1^2 h_1^4 + E_1 E_2 h_1 h_2 (4h_1^2 + 6h_1 h_2 + 4h_2^2) + E_2^2 h_2^4}{E_1 h_1 + E_2 h_2}.$$

K. SANLITURK and H. KORUK in [26, 27] proposed an alternative, more general method for finding the position of the  $z_0$  reference axis.

It is easy to check that if  $E_1 = E_2 = E$ , then  $z_0 = 0$ ,  $h_1 = h_2 = h/2$ , and the value of the moment of inertia is expressed by formula (2.2). Formula (2.23) defining  $(EI)_{eff}$  does not depend on the choice of the starting point of the  $z$  axis ( $z = 0$ ). Changing the starting point results in the change of the numerical value  $z_0$ , so that this point will always lie in the same place with respect to the geometry of the beam. The eigenfrequencies can be determined by inserting the effective quantities (2.23) and (2.9) into the formula (2.1):

$$(2.24) \quad f_i = \frac{\gamma_i}{\sqrt{12}} \frac{h_2}{l^2} \sqrt{\frac{E_1^2 \frac{h_1^4}{h_2^4} + E_1 E_2 \frac{h_1}{h_2} (4 \frac{h_1^2}{h_2^2} + 6 \frac{h_1}{h_2} + 4) + E_2^2}{(E_1 \frac{h_1}{h_2} + E_2) (\rho_1 \frac{h_1}{h_2} + \rho_2)}}.$$

By measuring the resonance frequencies for the two thicknesses  $h_2$  and  $h'_2$ , two equations are obtained, from which the Young's moduli  $E_1$  and  $E_2$  are then determined. These equations are not linear with respect to Young's modulus, as is the case for a symmetrical three-layer composite, and therefore their solution is more difficult. Similarly, as in the PM1 method, in this paper the two values of  $h_2$  and  $h'_2 = 2h_2$  were chosen. Condition (2.17) must also be met, as in the PM1 method.

The expression from which the loss factor can be determined is also more complex. Taking the composite form of Young's modulus and omitting expressions of orders higher than the first with respect to the loss factors  $\eta_1$  and  $\eta_2$ , the result is:

$$(2.25a) \quad \text{Re}(\underline{EI}) = \frac{G}{(E_1 h_1 + E_2 h_2)^2},$$

$$(2.25b) \quad \text{Im}(\underline{EI}) = \frac{E_1 h_1 [E_1^2 h_1^4 + 2E_1 E_2 h_1^3 h_2 + E_2^2 h_2^2 (4h_1^2 + 6h_1 h_2 + 3h_2^2)]}{(E_1 h_1 + E_2 h_2)^2} \eta_1 \\ + \frac{E_2 h_2 [E_2^2 h_2^4 + 2E_1 E_2 h_1 h_2^3 + E_1^2 h_1^2 (3h_1^2 + 6h_1 h_2 + 4h_2^2)]}{(E_1 h_1 + E_2 h_2)^2} \eta_2.$$

The quotient of the imaginary part (2.25b) and the real part (2.25a) of the quantity  $\underline{EI}$  is the effective damping factor:

$$(2.26a) \quad \eta_{eff} = \frac{\text{Im}(\underline{EI})}{\text{Re}(\underline{EI})} = \alpha \eta_1 + \beta \eta_2,$$

$$(2.26b) \quad \alpha = \frac{E_1 h_1 [E_1^2 h_1^4 + 2E_1 E_2 h_1^3 h_2 + E_2^2 h_2^2 (4h_1^2 + 6h_1 h_2 + 3h_2^2)]}{G},$$

$$(2.26c) \quad \beta = \frac{E_2 h_2 [E_2^2 h_2^4 + 2E_1 E_2 h_1 h_2^3 + E_1^2 h_1^2 (3h_1^2 + 6h_1 h_2 + 4h_2^2)]}{G},$$

where

$$G = E_1^3 h_1^5 + E_1 E_2 h_1 h_2 (5E_1 h_1^3 + 6E_1 h_1^2 h_2 + 4E_1 h_1 h_2^2 \\ + 4E_2 h_1^2 h_2 + 6E_2 h_1 h_2^2 + 5E_2 h_2^3) + E_2^3 h_2^5.$$

This is a linear equation with respect to  $\eta_1$  and  $\eta_2$ . By measuring the effective loss factors for two different layer thicknesses and having Young's modulus determined on the same basis, a system of two linear equations from which the loss factors  $\eta_1$  i  $\eta_2$  can be extracted is obtained.

It must be pointed out that both  $E$  and  $\eta$  are frequency dependent. Therefore, in order to obtain results for different frequencies, one has to alter the beam length or measure different bending modes.

### 3. Numerical validation

A numerical validation of the methods derived in the previous part of the article was carried out. For this purpose, a virtual FEM model of the composite was developed in Comsol Multiphysics software. The prepared model was equivalent to a composite that was also tested in the laboratory (dimensions of the samples can be found in Table 5). The composite consisted of a steel beam as the core, and rubber as the shell. Four different variations of the model were developed in order to test methods O, MO, PM1 and PM2. An example of the developed model is shown in Fig. 4.

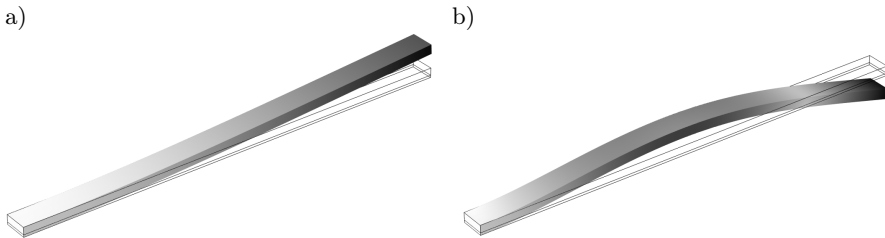


FIG. 4. FEM model, variant for testing method O; a) 1st mode of the composite vibration (20.4 Hz), b) 2nd mode of the composite vibration (128.0 Hz).

Young's modulus and the loss factor entered into the model was an average value obtained from measurements (a description of the course of measurements and other beam parameters are presented in part 4 of the paper). The adopted values  $E$  and  $\eta$  are summarized in Table 1. Those assumed values of  $E$  and  $\eta$  are further referenced as VATM (value assigned to the model).

TABLE 1.  $E$  and  $\eta$  parameters used for the FEM modelling.

Layer	Young's modulus, $E$ [GPa]	Loss factor, $\eta$ [-]
Steel (core)	1.91E+02	0.00315
Rubber (sheathing)	3.50E-02	0.89000

The validation consisted of 2 stages. The first stage involved comparing the rubber parameters  $E_2$ ,  $\eta_2$  extracted by methods O, MO, PM1 and PM2, with the values being directly entered into the model (Table 1). The performance of the PM1 and PM2 methods in determining the core parameters  $E_1$  and  $\eta_1$

in comparison with the direct measurement was also evaluated. At this stage, any uncertainties associated with the preparation of the composite samples were eliminated, as the adopted geometry was ideal. Stage 2, on the other hand, involved estimating the effect of sample precision on the obtained results.

### 3.1. Influence of the applied method

The analysis consisted of FEM simulations in the frequency domain to determine the resonance curves of the test specimens. The specimen was excited uniformly across the surface from one side, while from the other side of the specimen the response (vibration velocity) averaged across the beam was collected. This allowed for the reading of the natural frequencies and the widths of the resonance curves. The remaining procedure was carried out as described in the theoretical part of this article (implementing equations of methods O, MO, PM1, and PM2). Parameters of steel have also been determined by performing a direct virtual measurement on a bare steel beam without any sheathing (standardized method). Finally, it was possible to assess the accuracy of mathematical models by computing a relative error of  $E$  and  $\eta$ . The error was calculated in relation to the true value assigned to the model (VATM). The analysis was performed for 1 and 2 modes of vibrations. The obtained steel and rubber parameters are summarized in Tables 2 and 3, respectively. The obtained results indicate that the tested methods, even in ideal conditions, do not allow the real parameters of the materials forming the composite to be reproduced with an infinitely high precision.

TABLE 2. Steel parameters determined by virtual FEM and their errors with respect to VATM.

Method	1st resonance				2nd resonance			
	$E_1$		$\eta_1$		$E_1$		$\eta_2$	
	value [GPa]	error	value [-]	error	value [GPa]	error	value [-]	error
VATM	1.91E+02	0.0%	0.00315	0.0%	1.91E+02	0.0%	0.00315	0.0%
PM1	1.92E+02	0.5%	0.00405	28.4%	1.92E+02	0.7%	-0.00112	-135.7%
PM2	1.93E+02	0.9%	0.00377	19.7%	1.93E+02	0.9%	0.00348	10.4%
Direct	1.93E+02	1.0%	0.00314	-0.4%	1.93E+02	1.0%	0.00314	-0.3%

The highest precision in determining the sheathing parameters was shown by PM2 for the 2nd resonance, where an error of 2.3% in the determination of Young's modulus and an error of -0.5% in the determination of the loss factor were obtained. The lowest precision in the determination of the sheathing parameters was shown by PM1 for the 1st resonance, where an error of 14.9% in the determination of  $E_2$ , and an error of -10.7% in the determination of  $d_2$  was obtained.

TABLE 3. Rubber parameters determined by virtual FEM and their errors with respect to VATM.

Method	1st resonance				2nd resonance			
	$E_2$		$\eta_1$		$E_2$		$\eta_2$	
	value [GPa]	error	value [-]	error	value [GPa]	error	value [-]	error
VATM	3.50E-02	0.0%	0.89	0.0%	3.50E-02	0.0%	0.89	0.0%
O	3.74E-02	6.9%	0.96	8.3%	3.53E-02	0.9%	1.01	13.4%
MO	3.75E-02	7.1%	0.91	2.5%	3.61E-02	3.2%	0.94	5.7%
PM1	4.02E-02	14.9%	0.79	-10.7%	3.74E-02	6.7%	0.93	4.1%
PM2	3.84E-02	9.7%	0.83	-6.9%	3.58E-02	2.3%	0.89	-0.5%

For the determination of the core parameters, it is best to use the direct method, as it gives the lowest errors in both the determination of  $E_1$ , and  $\eta_1$ .

### 3.2. Influence of sample precision

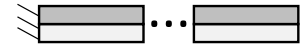
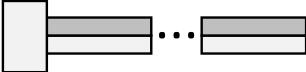
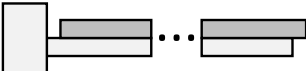
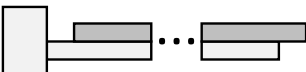
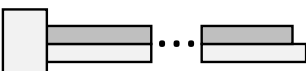
The analysis of the influence of sample precision involved the same steps as the analysis of the influence of the method used. However, it was limited to method O and the first vibration mode only. In this step, intentional errors were introduced into the system geometry to reproduce situations that might occur during a real measurement situation. In particular, the influence of an inaccurate rubber cut-out (increments  $\Delta l$ ) on both the immobilized side and on the free side of the beam was evaluated. The differences between ideal immobilization of the beam edge and the use of a steel cube on the beam edge were also checked. The steel cube resembled the cube used in real measurements (see Fig. 5) and it allowed a slight movement of the beams at the “fixed” end. It was modelled as an additional FEM linear elastic material made of steel.



FIG. 5. Examples of the tested steel-core composites.

Obtained Young's moduli and rubber loss factors are summarized in Table 4. From Table 4 it can be concluded that the largest errors occur when the sample is inaccurately made near the free edge of the composite (errors can then exceed even 100%). In contrast, the introduction of a steel cube did not significantly change the obtained viscoelastic parameters when compared to the use of an ideal boundary condition.

TABLE 4. Influence of the precision of cutting out and attaching the shell to the core on the determined viscoelastic parameters.

No.	Sketch	$\Delta l$ , clamped end [mm]	$\Delta l$ , free end [mm]	Rubber parameters		Error	
				$E_2$ [GPa]	$\eta_2$ [-]	$E_2$	$\eta_2$
1	Values assigned to the model	–	–	3.50E-02	0.89	0%	0%
2		0	0	3.74E-02	0.96	7%	8%
3		0	0	3.68E-02	0.98	5%	10%
4		–1	+1	2.34E-02	1.35	–33%	52%
5		–2	+2	1.38E-02	2.24	–61%	151%
6		0	–1	4.58E-02	0.79	31%	–11%
7		0	–2	5.47E-02	0.67	56%	–25%
8		–1	0	3.22E-02	0.99	–8%	11%
9		–2	0	3.21E-02	0.98	–8%	10%
10		0	+1	2.82E-02	1.27	–19%	43%
11		0	+2	1.98E-02	1.80	–44%	102%

## 4. Tested materials and measurement methods

### 4.1. The measured composite beams

Table 5 summarizes basic information about the tested composites, and Fig. 5 shows examples of the composite beams used in the measurements.

TABLE 5. Parameters of the tested composites.

No.	Core	$\rho_1$ [kg/m <sup>3</sup> ]	$h_1$ [mm]	Sheathing	$\rho_2$ [kg/m <sup>3</sup> ]	$h_2$ [mm]	$l$ [cm]
1	Steel	7827	1	rubber	1359	3 or 6 (PM2) 6 or 12 (PM1)	18.0
2	PVC	1408	2	rubber	1359	3 or 6 (PM2) 6 or 12 (PM1)	13.0

Rubber cut from a 3 mm thick sheet was used as the test material. To ensure that the parameters of the rubber of different  $h_2$  thicknesses were the same, two thicknesses of the same rubber were used: 3 mm (on both sides for the PM1 method, or on one side for the PM2 method), or 6 mm (on both sides or on one side). In the latter case, two sheets of rubber were glued together. When assembling the composites, care was taken to ensure that the layer of adhesive used was as thin as possible. The prepared configurations of the beams allowed for the comparison of the O, MO, PM1, and PM2 methods, and also the assessment of the influence of the type of adhesive (cyanoacrylate, epoxy, butaprene) and core material (steel, PVC). For each tested variant, 5 identical composite samples were made in order to determine the mean value and standard deviation. The lengths of the steel and PVC beams were chosen so that resonances in similar frequency ranges could be obtained.

### 4.2. Measurement stand and experiments

The measurements were made for a beam that was rigidly clamped at one end to the stand, as shown in Fig. 6. The measurement setup met the requirements of ASTM E756-05 [13]. The free end of the beam was vibrated by the BrüelKjær MM0002 non-contact electromagnetic actuator. The excitation was a sinusoidal signal with an amplitude of 10 V that was swept logarithmically in a given frequency range. Beam vibrations were recorded using the Polytec PSV400M2 laser vibrometer. With the help of the vibrometer, the frequency response of the vibration velocity was analyzed using the 6400 lines FFT. The VD-07 speed decoder, with a resolution of  $0.02 \mu\text{m/s}/\sqrt{\text{Hz}}$ , was used. To eliminate noise, four times averaging was used for each measurement. The vibrations of the beam were measured in its center and at a distance of about 3/4 of the length of the beam from the rigid clamp. The measurements were carried out at room temperature (about 22°C).

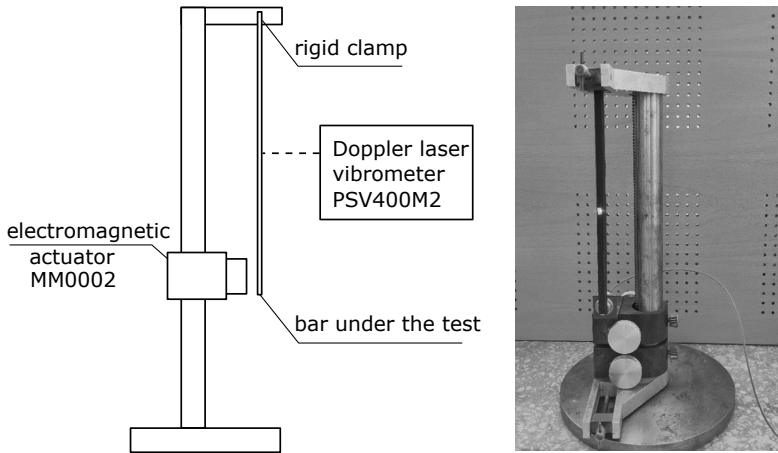


FIG. 6. Measurement setup.

The smallest frequency change that was possible with the laser vibrometer was 0,015262 Hz. This frequency resolution around the resonance curve was too low to accurately determine the loss factor. However, the measurements were not noisy, so an interpolation of the resonance curves with third order splines was used. An example of the measurement result and the approximation is shown in Fig. 7a. Figure 7b represents the full exemplary resonance curve.

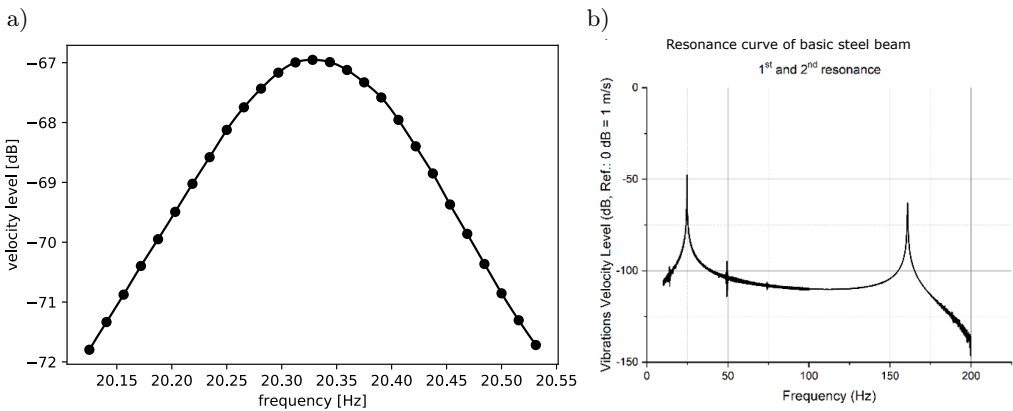


FIG. 7. a) Example of the resonance curve measurement result (black dots) and third-order spline approximation (solid line), b) Exemplary resonance curve of basic steel beam with 1st and 2nd resonance.

## 5. Results of measurements and discussion

In this section, the results obtained by the proposed methods (PM1 and PM2) are compared with the ASTM models (O and MO). Only two bending modes are investigated, because of low signal to noise ratio in the frequency response at higher frequencies. Results are shown for all measured samples. Each sample is labeled with a number ( $0, 1, \dots, N$ ). The absence of a marker in the graphs presented in this section of the article means that there is no measurement available for that sample. There is a significant scatter in the presented results between both the samples and the methods. However, the discrepancies obtained are very similar to those obtained during the numerical validation of the model, where the effect of sample preparation accuracy on the results was checked. This means that the scatter seen in the graphs is a characteristic feature of the resonance methods.

### 5.1. Base beam material parameters

Figure 8 shows determined Young's moduli, while Fig. 9 shows the loss factors of the cores (steel and PVC). Tables 6 and 7 summarize the mean values and standard deviations. In Figs. 8 and 9, outliers were intentionally left out to

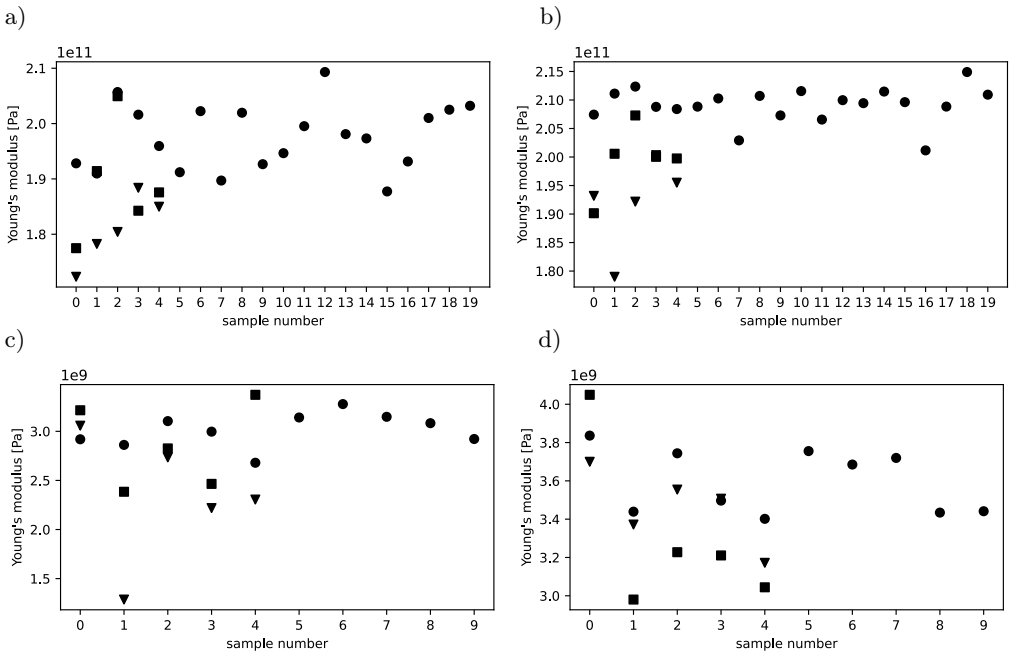


FIG. 8. Young's moduli of the core for all the tested samples,  $\nabla$  – PM1,  $\blacksquare$  – PM2,  $\bullet$  – direct measurement; a) steel, 1st resonance, b) steel, 2nd resonance, c) PVC, 1st resonance, d) PVC, 2nd resonance.

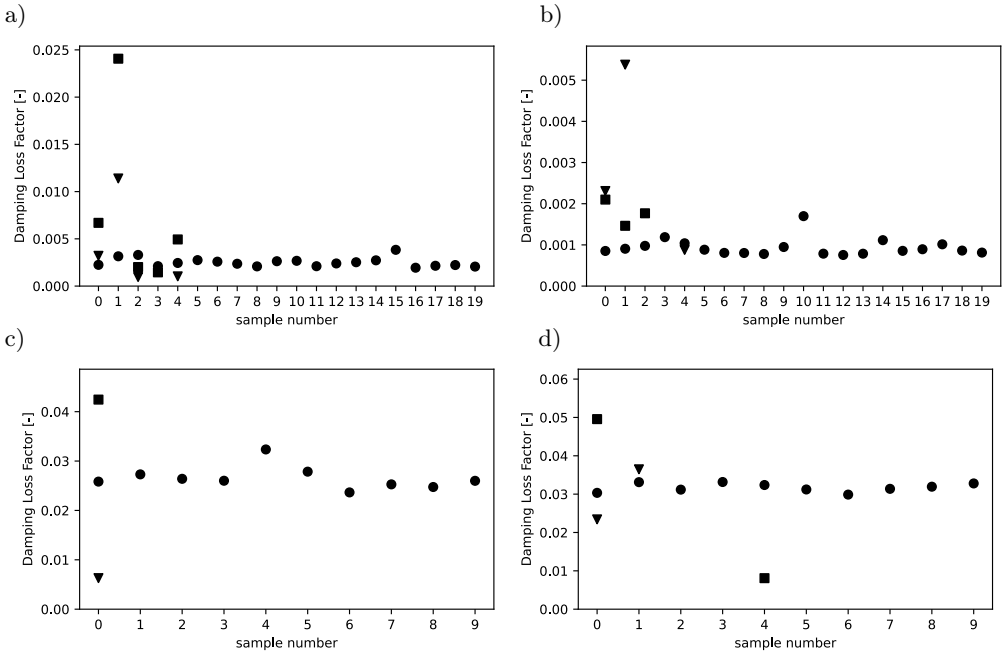


FIG. 9. Core loss factor for all the tested samples,  $\blacktriangledown$  – PM1,  $\blacksquare$  – PM2,  $\bullet$  – direct measurement; a) steel, 1st resonance, b) steel, 2nd resonance, c) PVC, 1st resonance, d) PVC, 2nd resonance.

illustrate the scatter of the results and were also ignored when determining the mean value and standard deviation. Parameters of steel have been determined indirectly using the proposed methods: PM1 and PM2 and by performing direct measurement on a bare steel beam without any sheathing (standardized method). The obtained results show that direct measurement of the mechanical properties of the core gives far more consistent results when compared to the proposed methods.

TABLE 6. Young’s modulus of the core material measurement statistics – mean value (standard deviation).

Young modulus, $E$ [GPa]						
Material	PM1		PM2		Direct measurement	
	1 res.	2 res.	1 res.	2 res.	1 res.	2 res.
Steel	1.81E+02 (6.20E+00)	1.92E+02 (7.94E+00)	1.89E+02 (1.02E+01)	2.00E+02 (6.12E+00)	1.98E+02 (5.87E+00)	2.09E+02 (3.10E+00)
PVC	2.58E+00 (3.91E-01)	3.46E+00 (2.00E-01)	2.85E+00 (4.39E-01)	3.30E+00 (4.31E-01)	3.01E+00 (1.73E-01)	3.60E+00 (1.67E-01)

TABLE 7. Table 7. Core loss factor measurement statistics – mean value (standard deviation).

Material	Loss factor, $\eta_2$ [-]					
	PM1		PM2		Direct measurement	
	1 res.	2 res.	1 res.	2 res.	1 res.	2 res.
Steel	1.73E-03 (1.28E-03)	1.59E-03 (1.01E-03)	3.77E-03 (2.47E-03)	1.78E-03 (3.18E-04)	2.52E-03 (4.75E-04)	9.38E-04 (2.14E-04)
PVC	6.29E-03 (-)	2.99E-02 (9.23E-03)	4.24E-02 (-)	2.88E-02 (2.93E-02)	2.65E-02 (2.36E-03)	3.17E-02 (1.14E-03)

## 5.2. Influence of glue type

A study of the effect of the type of adhesive on the identification of rubber parameters was only carried out for method O on the steel beam. Figure 10 shows determined Young's moduli, while Fig. 11 shows the loss factors. Table 8

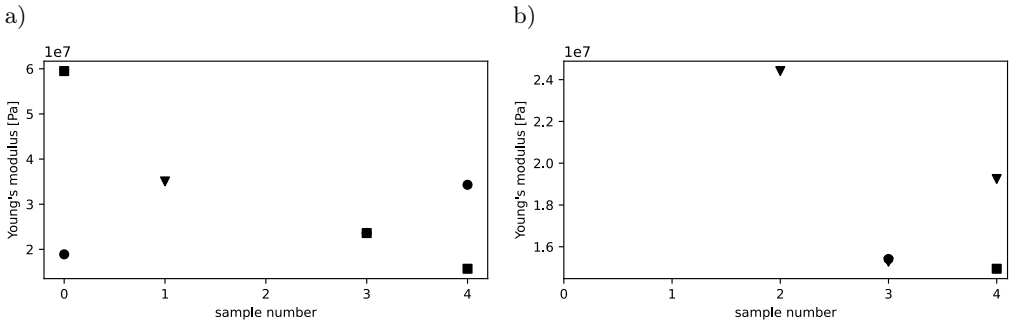


FIG. 10. Young's modulus of the rubber with regards to the adhesive of all the tested specimens (steel core, method O), ▼ – cyanoacrylate adhesive, ■ – butaprene, ● – epoxy adhesive; a) 1st resonance, b) 2nd resonance.

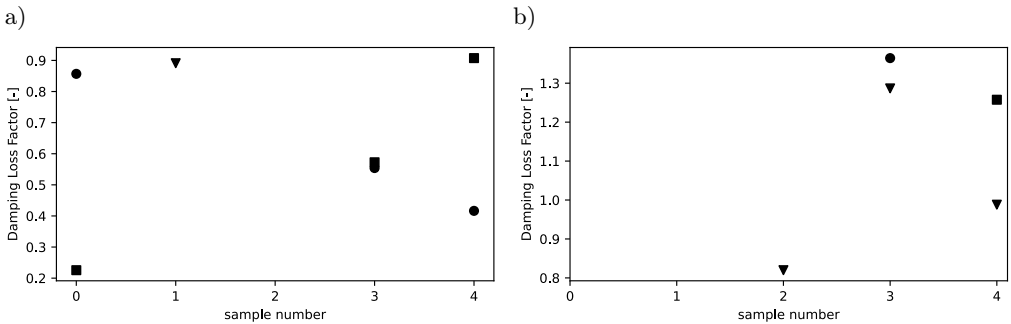


FIG. 11. Rubber loss factor in relation to the adhesive used for all the tested samples (steel core, method O), ▼ – cyanoacrylate adhesive, ■ – butaprene, ● – epoxy adhesive; a) 1st resonance, b) 2nd resonance.

TABLE 8. Measurement statistics: Young's modulus and loss factor with regards to the used adhesive – mean value (standard deviation).

Type of adhesive	$E$ [GPa]		$\eta$ [-]	
	1st resonance	2nd resonance	1st resonance	2nd resonance
Cyanoacrylate	3.50E-02 (-)	1.96E-02 (4.58E-03)	0.89 (-)	1.03 (0.24)
Butaprene	3.29E-02 (2.33E-02)	1.49E-02 (-)	0.57 (0.34)	1.26 (-)
Epoxy	2.56E-02 (7.89E-03)	1.54E-02 (-)	0.61 (0.23)	1.36 (-)

summarizes the mean values and standard deviations. It can be seen from the figures that only a small proportion of the measurements were not affected by numerical errors. All the samples with a large numerical error were simultaneously associated with a failure to fulfil condition (2.16b). Attention is drawn to the very large values of the loss factor obtained with the O method. Similar large values are also be shown for the MO method later in the paper.

Theoretical models explaining the influence of the adhesive on the viscoelastic parameters were not developed for this publication (any interested readers should refer to [28]).

### 5.3. Influence of the base beam material

Figure 12 shows Young's moduli, while Fig. 13 shows the rubber loss factors determined by all the tested methods. Tables 9 and 10 summarize the mean values and standard deviations. The following relationships were observed:

For methods O and MO, measurement on a core made of PVC generally results in the determination of higher values of  $E_2$  and smaller values of  $\eta_2$  when compared to the measurement on the steel core. For the PM1 and PM2 methods, measurement on a PVC core generally results in smaller values of  $E_2$  and higher values of  $\eta_2$  when compared to the measurement on the steel core.

Note that in Figs. 12 and 13, all markers for PM1 and PM2 are present. It means that for each sample, a result that is a positive number is obtained. Conversely, some markers describing O and MO are missing because a negative value of  $E$  or  $\eta$  was obtained, and this result is not plotted in the graph. A numerical error (missing values) from O and MO were present for those samples where the criterion described by an inequality (2.6) was not met. On the other hand, samples used in the PM1 method fulfilled the equivalent criterion (2.15c), and no numerical errors were present. In this article, we did not derive the criterion for the PM2 method, but one can see in the graph that no PM2 samples providing

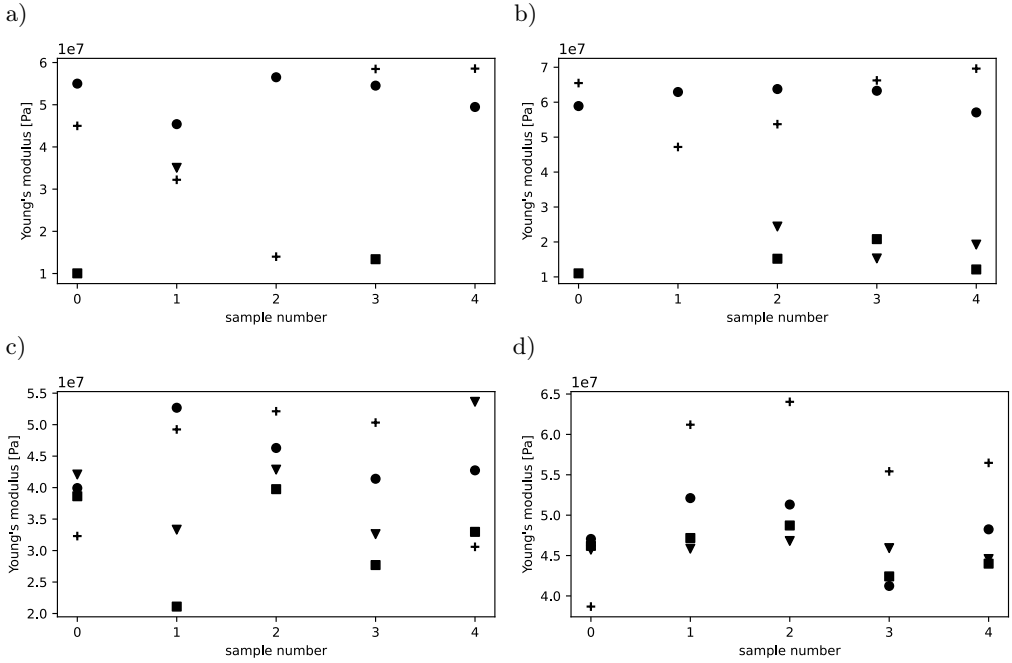


FIG. 12. Young's modulus of the rubber determined by all the tested methods,  $\blacktriangledown$  – O,  $\blacksquare$  – MO,  $\bullet$  – PM1,  $+$  – PM2; a) steel, 1st resonance, b) steel, 2nd resonance, c) PVC, 1st resonance, d) PVC, 2nd resonance.

negative values are present. This clearly shows the advantage of the proposed methods. Experiments showed that it is less troublesome to meet (2.15c) criterion than (2.6). This directly translates into the fact that using PM1 and PM2 ap-

TABLE 9. Statistics of measuring the rubber's Young's modulus with regards to the used method – mean value (standard deviation).

Method	Young modulus, $E$ [GPa]			
	Steel		PVC	
	1st resonance	2nd resonance	1st resonance	2nd resonance
O	3.50E-02 (-)	1.96E-02 (4.58E-03)	4.09E-02 (8.56E-03)	4.58E-02 (7.97E-04)
MO	1.17E-02 (2.37E-03)	1.48E-02 (4.39E-03)	3.20E-02 (7.78E-03)	4.57E-02 (2.51E-03)
PM1	5.22E-02 (4.62E-03)	6.12E-02 (3.01E-03)	4.46E-02 (5.09E-03)	4.80E-02 (4.32E-03)
PM2	4.16E-02 (1.89E-02)	6.04E-02 (9.54E-03)	4.29E-02 (1.05E-02)	5.52E-02 (9.86E-03)

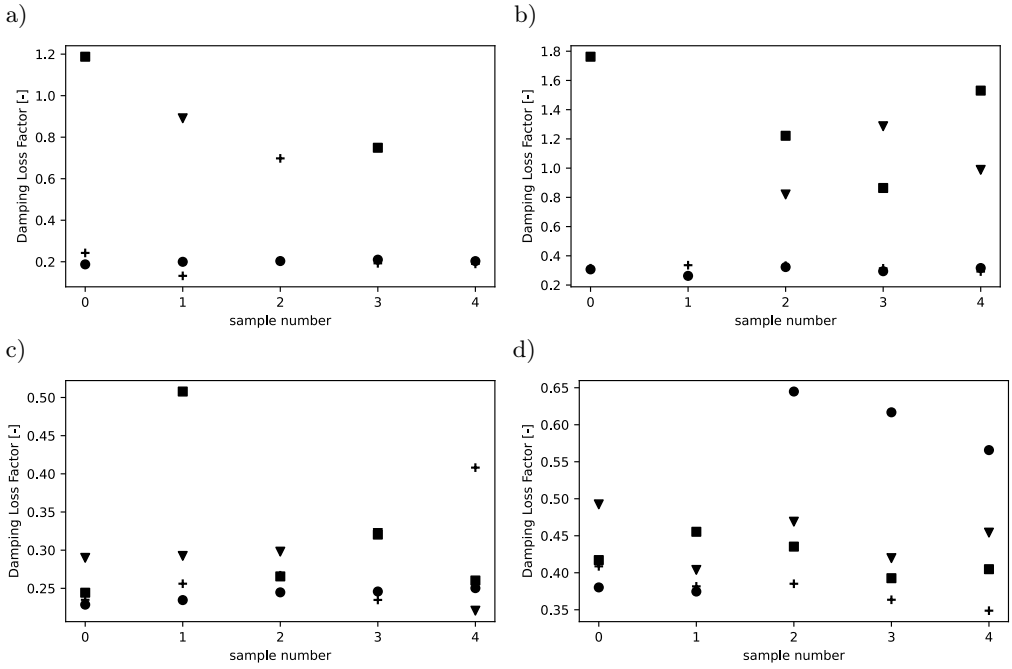


FIG. 13. Rubber loss factor determined by all the tested methods,  $\blacktriangledown$  – O,  $\blacksquare$  – MO,  $\bullet$  – PM1,  $+$  – PM2; a) steel, 1st resonance, b) steel, 2nd resonance, c) PVC, 1st resonance, d) PVC, 2nd resonance.

proaches allows for obtaining physically meaningful results using fewer samples. The disadvantages of the proposed methods can be seen to be the more time-consuming sample preparation and the more complicated mathematical model. Moreover, when the aim is to determine the mechanical parameters of the core itself, an improvement of numerical properties does not occur (and they even deteriorate).

TABLE 10. Statistics of measuring the rubber's loss factor with regards to the used method – mean value (standard deviation).

Loss factor, $\eta$ [-]				
Method	Steel		PVC	
	1st resonance	2nd resonance	1st resonance	2nd resonance
O	0.89 (-)	1.03 (0.24)	0.28 (0.04)	0.45 (0.04)
MO	0.97 (0.31)	1.34 (0.39)	0.32 (0.11)	0.42 (0.02)
PM1	0.20 (0.01)	0.30 (0.02)	0.24 (0.01)	0.52 (0.13)
PM2	0.29 (0.23)	0.32 (0.02)	0.28 (0.07)	0.38 (0.02)

## 6. Conclusions

This paper presents and validates two new methods of determining the viscoelastic parameters of materials. The viscoelastic parameters were determined by twice measuring the frequency response of a composite beam with different layer thickness ratios. In this paper, the ratio of these thicknesses was equal to 2.

The main advantage of the proposed methods is the easy fulfilment of the conditions necessary for the existence of a sensible solution insensitive to measurement errors, i.e. the condition given by Eq. (2.17), while for the methods described in the ASTM standard, the non-fulfilment of the analogous condition (2.16b) is relatively frequent. The PM1 method fulfilled the criterion in 100% cases, while O and MO methods in total fulfilled the criterion only in 65% cases. In the 35% cases, where the criterion was not met, the negative values of loss factors and Young's modulus have been obtained, which is obviously an measurement error. Those results were rejected when calculating average values of Young's modulus and loss factors.

The disadvantages of the proposed methods can be seen to be the more time-consuming sample preparation and the more complicated mathematical model. Moreover, when the aim is to determine the mechanical parameters of the core itself, an improvement of numerical properties does not occur (and they even deteriorate). Also, the possible improvement of the method could be performing tests with many different thickness ratios and finding the optimal solution using minimization algorithms. Taking into account the mention disadvantages, a reasonable strategy to measure viscoelastic parameters is to carry out measurements with standard methods, and then possibly to switch to new methods if numerical problems occur.

If the aim is to determine the mechanical parameters of the core, more consistent results can be obtained by using the direct method instead of the PM1 and PM2 methods, as was confirmed by both the simulations and measurements.

The simulations suggest that the PM2 method used for the 2nd resonance of the sample may be the most accurate of all the tested methods.

It was noted that in the case of the PM1 and PM2 methods, the use of a core with a relatively low Young's modulus can underestimate determined Young's modulus and overestimate the sheath loss factor. All the tested methods require very precise manufacturing of the test specimens. The specimens should be of high quality, especially near the free edge of the beam. However, even then, the tested methods have limited accuracy, which was shown by the FEM simulations. When the errors related to the precision of the specimens are significant, only an approximate determination of the viscoelastic parameters (with an accuracy of about one order of magnitude) is possible.

## Acknowledgements

The work was financially supported by the Department of Acoustics, Multimedia and Signal Processing, the Wrocław University of Science and Technology and KFB Acoustics sp. z o.o.

## References

1. T. LEE, R.S. LAKES, A. LAL, *Resonant ultrasound spectroscopy for measurement of mechanical damping: Comparison with broadband viscoelastic spectroscopy*, Review of Scientific Instruments, **71**, 2855–2861, 2000.
2. ASTM E1876-15, *Standard Test Method for Dynamic Young's Modulus, Shear Modulus, and Poisson's Ratio by Impulse Excitation of Vibration*, 2015.
3. K.P. MENARD, N.R. MENARD, *Dynamic mechanical analysis in the analysis of polymers and rubbers*, Encyclopedia of Polymer Science and Technology, 1–33, 2002.
4. R.E. WETTON, R.D.L. MARSH, J.G. VAN-DE-VELDE, *Theory and application of dynamic mechanical thermal analysis*, Thermochimica Acta, **175**, 1–11, 1991.
5. C.P. CHEN, R.S. LAKES, *Apparatus for determining the viscoelastic properties of materials over ten decades of frequency and time*, Journal of Rheology, **33**, 1231–1249, 1989.
6. J. PARK, J. LEE, J. PARK, *Measurement of viscoelastic properties from the vibration of a compliantly supported beam*, The Journal of the Acoustical Society of America, **130**, 3729–3735, 2011.
7. Y. LIAO, V. WELLS, *Estimation of complex modulus using wave coefficients*, Journal of Sound and Vibration, **295**, 165–193, 2006.
8. Y. LIAO, V. WELLS, *Estimation of complex Young's modulus of non-stiff materials using a modified Oberst beam technique*, Journal of Sound and Vibration, **316**, 87–100, 2008.
9. R.H. LYON, R.G. DEJONG, M. HECKL, *Theory and Application of Statistical Energy Analysis*, Newnes, Boston, 1995.
10. A.D. NASHIF, D.I.G. JONES, J.P. HANDERSON, *Vibration Damping*, John Wiley & Sons, New York, 1991.
11. M. BOLDUC, N. ATALLA, *Measurement of SEA damping loss factor for complex structures*, The Journal of the Acoustical Society of America, **123**, 3060–3060, 2008.
12. H. OBERST, K. FRANKENFELD, *Über die Dämpfung der Biegeschwingungen dünner Bleche durch fest haftende Beläge, About the damping of bending vibrations of thin sheets by firmly adhering linings*, Acta Acustica united with Acustica, **2**, 181–194, 1952.
13. H. KORUK, K.Y. SANLITURK, *Damping uncertainty due to noise and exponential windowing*, Journal of Sound and Vibration, **330**, 5690–5706, 2011.
14. D.J. EWINS, *Modal Testing: Theory, Practice and Application*, John Wiley & Sons, New York, 2009.
15. M.S. OZER, H. KORUK, K.Y. SANLITURK, *Testing non-magnetic materials using Oberst Beam Method utilising electromagnetic excitation*, Journal of Sound and Vibration, **456**, 104–118, 2019.

16. M.S. OZER, H. KORUK, K.Y. SANLITURK, *Characterization of viscoelastic materials using free-layered and sandwiched samples: assessment and recommendations*, Acta Physica Polonica A, **127**, 1251–1254, 2015.
17. H. KORUK, K.Y. SANLITURK, *On measuring dynamic properties of damping materials using Oberst Beam Method*, ASME 2010 10th Biennial Conference on Engineering Systems Design and Analysis ESDA2010, 127–134, 2010.
18. N. JADE, S. BHIRODKAR, B. VENKATESHAM, *Measurement of damping properties of beeswax and cosmetic wax using oberst beam method*, Vibroengineering Procedia, **29**, 54–59, 2019.
19. ASTM E756-9804, *Standard Test Method for Measuring Vibration-Damping Properties of Materials E756-9804*, 1–18, 2017.
20. ISO 18437-2:2005, *Mechanical vibration and shock — Characterization of the dynamic mechanical properties of visco-elastic materials — Part 2: Resonance method*, 2005.
21. SAE J1637, *Laboratory Measurement of the Composite Vibration Damping Properties of Materials on a Supporting Steel Bar*, 2022.
22. H. KORUK, K.Y. SANLITURK, *Identification and removal of adverse effects of non-contact electromagnetic excitation in Oberst Beam Test Method*, Mechanical Systems and Signal Processing, **30**, 274–295, 2012.
23. H. KORUK, *Quantification and minimization of sensor effects on modal parameters of lightweight structures*, Journal of Vibroengineering, **16**, 1952–1963, 2014.
24. J.L. WOJTOWICKI, L. JAOUEN, R. PANNETON, *New approach for the measurement of damping properties of materials using the Oberst beam*, Review of Scientific Instruments, **75**, 2569–2574, 2004.
25. ANSI/ASA S2.22-1998, *Resonance Method for Measuring The Dynamic Mechanical Properties of Viscoelastic Materials*, 1998.
26. K.Y. SANLITURK, H. KORUK, *Development and validation of a composite finite element with damping capability*, Composite Structures, **97**, 136–146, 2013.
27. K.Y. SANLITURK, H. KORUK, *A new triangular composite shell element with damping capability*, Composite Structures, **118**, 322–327, 2014.
28. F.P. MECHEL [ed.], *Formulas of Acoustics*, 2nd ed., Springer, Berlin, 2004.

Received July 12, 2022; revised version April 25, 2023.

Published online May 12, 2023.

---